Research article

Optimization of soluble phosphate and IAA production using response surface methodology and ANN approach

Yasin Ahmed Waday [a,*], Ermias Girma Aklilu [a], Mohammed Seid Bultum [a], Venkata Ramayya Ancha [b]

[a] *School of Chemical Engineering, Jimma Institute of Technology, Jimma University, Jimma 378, Ethiopia*
[b] *Faculty of Mechanical Engineering, Jimma Institute of Technology, Jimma University, Jimma 378, Ethiopia*

A R T I C L E   I N F O

A B S T R A C T

Phosphorus (P) is often found inaccessible to plants, as it forms precipitates with cations and can be converted to accessible forms by using Phosphate solubilizing bacteria (PSB). In the present study, isolation and characterization of PSB from rhizospheric soil of coffee plants were performed. The influence of four independent variables (incubation temperature, incubation time, pH, and inoculum size) was investigated and optimized using an artificial neural network and response surface methodology on the solubility of phosphate and indole acetic acid production. The bacterium that can dissolve phosphate were isolated in Pikovskaya's agar containing insoluble tricalcium phosphate. Total, six Phosphate Solubilizing Bacteria were isolated and three of them (PSB1, PSB3, and PSB4) were found to be effectively solubilizing phosphate. Based on phosphate solubilizing index results *Pseudomonas* bacteria (PSB1) was selected for modeling. The results showed that both models performed reasonably well, but properly trained artificial neural networks have the more powerful modeling capability compared to the response surface method. The optimum conditions were found to be incubation temperature of 37.5 °C, incubation time of 9 days, pH of 7.2, and inoculum size of 1.89 OD. Under these conditions, the model predicted solubility of phosphate of 260.69 μg/ml and production of IAA of 80.00 μg/ml with a desirability value of 0.947. In general, the isolated *Pseudomonas* is expected to have phosphorus-degrading ability that promotes plant growth, and further field experimental work is required to use this bacterial strain as biofertilizer, as an alternative to synthetic fertilizer.

1. Introduction

Phosphorus (P) is one of the essential macronutrients for all life forms to carry out different metabolic activities as it is an essential component of the most important energy compound ATP and nucleic acids (DNA and RNA). In plants, phosphorus helps in the process of photosynthesis, proper plant maturation, and stress mitigation (Kalayu, 2019). Phosphorus in soils can exist in both organic and inorganic forms; the inorganic forms of phosphorus have been calculated to account for 35–70 % of total P in soil (Sharon et al., 2016). Although, both organic and inorganic forms are present in sufficient concentration and solubility in soils is very low (Anzuay et al., 2017). Phosphorus always forms phosphate complexes with other compounds in soil. Because the fixation of inorganic phosphorus into insoluble complexes prevents these compounds from being absorbed by plants, both acidic and alkaline soils suffer from a severe deficiency. Phosphatic fertilizers are added to the soil in varying amounts to address the issue of P deficiency in various crops. However, shortly after application, a significant portion of the soluble forms of P fertilizers precipitate into an insoluble form, rendering them unavailable to plants (Muleta et al., 2013). According to Elhaissoufi et al. (2020) the excessive and repeated application of soluble P fertilizers can cause economic constraint as well as pose a serious threat to groundwater. To solve such problem, biofertilizers is a sustainable and eco-friendly to environmental protection and give nutrient to plant in a safe way when they needed.

The effect of process parameters on the phosphate solubilizing rhizobacteria isolated from rhizospheric soil of different plants have been studied by several researchers (Anbalagan and Krishnaswamy, 2017; Baliyan et al., 2021) however, to the best of our knowledge there was no report on the solubility of phosphate and the production of indole acetic acids (IAA) rhizosphere bacteria isolated from rhizospheric soil of coffee plant by coupling artificial neural network (ANN) and response surface

---

methodology (RSM). RSM is widely used in the optimization of chemical and physical processes that integrates mathematical modeling and experimental design. ANN has been widely used due to its suitability for modeling and simulation of various processes in real engineering applications (Aklilu, 2021). ANN does not require a mathematical description of the phenomena in the process, so the simulation of the complicated systems could be performed more efficiently (Yu et al., 2021). Compared with the RSM focusing on the statistical importance of the linear process parameters and their interactions via analysis of variance (ANOVA), ANN is more reliable in capturing the nonlinear relationship between the dependent variable and independent process variables. Although ANN is an efficient tool to predict and optimize any complex process parameters, it cannot guarantee the globally optimal solution (Banerjee et al., 2017).

In the present study, the combination of ANN and genetic algorithm can generate the relationship between the optimal input operating variables and the output process under study. Subsequently, the result predicted by the ANN and RSM techniques were statistically compared, using various parameters, such as coefficient of determination (R^2), root means square error (RMSE), mean absolute error (MAE), standard error of prediction (SEP), mean of squared errors (MSE) and absolute average relative deviation (AARD) based on the validation data set for their predictive and generalization capabilities.

The phosphate-solubilizing ability and production of IAA of isolated bacteria were designed by response surface statistical experimental method using central composite design (CCD) was selected to establish the regression model. This study characterizes the microorganisms at the morphological and phenotypic levels. This study was conducted to investigate the effect of four parameters (incubation temperature, incubation time, pH, and inoculum size) on the solubility of phosphate and production of IAA and to optimize these processes variables by employing RSM and ANN. The interaction effect of the independent variables with the dependent variables using the response surface plots was illustrated. Meanwhile, the back-propagation ANN model was also developed and the optimal number of hidden neurons was determined by the trial and error method. The predictive abilities and modeling competencies of the two models are compared and confirmed.

2. Materials and methods

2.1. Soil samples collection and isolation of rhizobacteria

The study sites were located in Jimma Zone, Oromia regional state, in the southwestern part of Ethiopia. Jimma town is the capital and administrative center of the zone, located 346 km away from the capital city of Ethiopia. The town's geographical coordinates are approximately 7°41′ N latitude and 36° 50′E longitude with annual maximum and minimum temperature of 30 °C and 14 °C respectively (Alemu et al., 2011). The soil used for bacterial isolation was excavated from the 15–20 cm depth of roots of coffee and collected in sterilized plastic bags. The samples were stored at 4 °C in a refrigerator until the time of analysis.

Isolation of rhizosphere bacteria was done based on (Somasegaren and Hoben, 1994) method. In this method, 1 g of soil sample was transferred in 9 ml of sterilized distilled water and mixed by vortex shaker for 20 s. The suspension then diluted up to 10^{-9} dilutions. From each dilution, 0.1 ml of the diluted sample was poured onto a sterilized surface plate of nutrient agar (NA) medium supplemented with 100 μg/ml of cycloheximide to defeat fungal growth. Finally, the plate was incubated at 30 °C for 5days (Midekssa et al., 2015). Individual bacterial isolates on nutrient agar were further sub-cultured on the PVK agar medium (containing (g/l) glucose (10), Ca₃(PO₄)₂ (5), (NH₄)₂SO₄ (0.5), NaCl (0.2), MgSO4_7H₂O (0.1), KCl (0.2), yeast extract (0.2), MnSO₄.7H₂O and FeSO₄.7H₂O (0.0003 each), and agar (15)) to obtain a pure culture by streak plate method. Highly grown bacteria culture on PVK agar media was maintained at 4 °C in the refrigerator for further analysis and studies. All of the experiments were done aseptically to disinfect unnecessary microbes.

2.2. Characterization of the isolate

2.2.1. Morphological characterization of the isolates

Morphological characteristics such as shape, color, edge, motility, and endospores formation, and gram stain of the colony were examined according to (Isenberg, 1998) method.

2.2.2. Phenotypic identification of bacteria isolates

Indole test, Urease test, Catalase test, Voges-Proskauer (VP) test, Methyl Red (MR) test, and Citrate test of the isolated bacteria were conducted according to Bergey's manual of systematic bacteriology (Holt, 1994).

2.2.3. Determination of phosphate solubilization index (PSI)

Qualitative estimation of phosphate solubilization was conducted using plate assays on PVK agar. Phosphate solubilization indicated by development of clear zone around a growing colony and this determined by calculation of PSI through Eq. (1) (Pande et al., 2017).

$$PSI = \frac{\text{Total diameter (colony + halo zone)}}{\text{colony diameter}} \tag{1}$$

2.3. P-solubilization efficiency of isolate in broth media

The isolated bacteria with the highest PSI were chosen, and the isolate's quantitative phosphate solubilization efficiency was measured in modified PVK broth media (Pande et al., 2017). The isolate (500 μl) was inoculated into 100 ml PVK broth media in 250 ml conical flask containing 5 g/l insoluble phosphates in the form of tricalcium phosphate (TCP) and incubated on a shaker incubator at 120 rpm for incubation temperature (25–45 °C), incubation time (3–15 days), pH (5–9) and inoculum size (1–3 OD). The process variables ranges were selected based on (Baliyan et al., 2021; Mohd Yusoff et al., 2017). Five ml of samples were withdrawn from each treatment and analyzed for phosphorus solubilization.

2.4. Quantification of soluble phosphorus

The phosphorus in the supernatant was determined according to (Watanabe and Olsen, 1965). The withdrawn samples were centrifuged at 15,000 rpm for 15 min and were filtered through 0.2 mm filter paper. 0.1 ml of the filtered supernatant was mixed with 0.25 ml of Barton's reagent, and the volume was increased to 5 ml using distilled water. The optical density (OD) of the supernatant was measured with a spectrophotometer at a wavelength of 700 nm after 10 min, and the amount of P-solubilized by strain was extrapolated from the standard curve. To perform standard curve, a stock P solution was made by dissolving 0.02195 g of KH2PO4 in 1L distilled water. A 20 ml dilution of the stock solution was collected, and the volume was increased to 30 ml using distilled water and labeled as the working solution. Each flask had a fraction of 0.2, 0.4, 0.8, 1.2, 2.0, 2.5, 3.0 ml of working solution and 0.25 ml of Barton's reagent, and the volume was increased to 5 ml with distilled water. The intensity of the yellow color formed after 10 min was measured spectrophotometrically at 700 nm. Plotting absorbance at 700 nm against P concentration yielded a standard curve.

2.5. Assay for indole-3-acetic acid (IAA) production

Quantitative production of IAA was determined using the colorimetric method as described by (Lebrazi et al., 2020). On a shaker incubator at 180 rpm, the bacterial isolates were cultured in Erlenmeyer flasks containing 50 mL of YMB supplemented with 0.1 percent DL-tryptophan, varying the incubation temperature (25–45 °C), incubation time (3–15 days), pH (5–9), and inoculum size (1–3 OD). Salkowski reagent was used to check the production of IAA following the centrifugation of the culture (Gordon and Weber, 1951). The resulting solution

was examined in a spectrophotometer at 530 nm and the concentration of IAA produced was estimated using a standard IAA curve and expressed in terms of µg/mL.

2.6. Experimental design and statistical analysis

The relation between different parameters was evaluated by the response surface statistical experimental method using the design expert software version of 11.1.2.06. This study was conducted using RSM, CCD by considering incubation temperature (A) and incubation time (B), pH (C) and, inoculum size (D) on solubilization of phosphate and IAA production. Generally, CCD involves sixteen factorial points, eight axial points, and six points at the center were carried out with a total of 30 experiments as shown in Eq. (2). All four factors have to be adjusted at five coded levels (-α, -1, 0, +1, + α). The relationship between the coded and the actual value of the variables is shown in Table 1. The variables were coded according to the equation:

$$N = 2^n + 2n + n_c = 2^4 + 2*4 + 6 = 30 \tag{2}$$

where N is the total number of experiments required, n is the number of variables, and n_c is the number of replicates.

The second-order polynomial multiple the quadratic regression equation was used to determine the relationship between independent variables and responses (Eq. (3)).

$$Y = b_o + \sum_{i=1}^{n} b_{i_i} X_i + \sum_{i=1}^{n} b_{ii} X_i^2 + \sum_{i=1}^{n-1} \sum_{j=i+1}^{n} b_{ij} X_i X_j + e_i \tag{3}$$

where Y is the experimental response (i.e., phosphate solubilization or IAA production), n is the number of independent variables, b_0 is the constant coefficient, b_i is the linear coefficient, b_{ij} is the second-order interaction coefficient, b_{ii} is the quadratic coefficient, e_i, x_i and x_j are the coded values of the independent variables. The coefficient of determination R^2, adjusted R^2, and predicted coefficient R^2, lack of fit from ANOVA, main effect of the regression were used in the determination of the quality of the developed model.

2.7. ANN modeling

The feed-forward architecture of ANN also known as multilayered perceptron (MLP) was selected to develop a predictive model with a layer of four neurons (incubation temperature, incubation time, pH, and inoculum size) as input, two layer of neurons (solubility of phosphate and IAA production) as output, and 10 hidden layer as indicted in Figure 1. 70% of the data points were selected for training to develop the neural network, 15% of the data set used for validation and 15% data sets for testing. The simple illustration of the ANN structure was shown in Figure 1. The number of neurons in the hidden layer were calculated from the following expression (Eq. (4)) (Aklilu 2021) (see Table 2).

$$2(n+m)^{0.5} \text{ to } 2n+1 \tag{4}$$

where n is the number of neurons in the input layer and m is the number of neurons in the output layer. Each network is trained separately, and therefore, the best network is selected based on the accuracy of the

predictions within the testing phase. The feed forward ANN in this study was trained using the Levenberg-Marquardt algorithm represented in Eq. (5). To achieve fast convergence to the minimum mean square error (MSE), the inputs and outputs are scaled within the uniform range of 0 (new x_{min}) to 1 (new x_{max}) by the following Eq. (5) to ensure uniform attention during the training process.

$$X_{normal} = \frac{X_i - X_{\min}}{X_{\max} - X_{\min}} (newX_{\max} + newX_{\min}) + newX_{\min} \tag{5}$$

where X_{norm} is the normalized data, X_i is the input/output data (data of independent and dependent variables), X_{max} and X_{min} are the maximum and minimum values of the particular variable, respectively. ANN Modeling using Toolbox of MAT LAB version 8.1 (R2013a) was applied to evaluate the goodness of fitting model using RSM data output.

2.8. Comparative analysis of RSM and ANN models

For this study, the performance of ANN and RSM were evaluated the goodness of the fitting and prediction accuracy of the constructed models by using the following error functions; RMSE, SEP, R^2, MAE, MSE, and AARD. The models were acceptable as R^2 was closer to the value of 1 and the other error function values were as small as possible (Monzón and Villanueva, 2021). The equations representing each error function are presented by Eqn. 6 to 11 (Table 2). To study the comparison of experimental with predicted values obtained by the RSM and ANN models, the values are tabulated and compared with the corresponding experimental values.

3. Results and discussion

3.1. Isolation and quantification of phosphate solubilization index (PSI)

In the present study, the rhizosphere bacteria was isolated from rhizospheric soil of coffee plants on NA medium supplemented with 100 µg/ml of cycloheximide. Individual bacterial isolates on nutrient agar were further sub-cultured on the PVK agar medium to evaluate in vitro for P solubilizing bacteria. A total of 6 phosphate solubilizing bacterial colonies were isolated on PVK agar medium, containing tricalcium phosphate (TCP) (see Table 3). Out of 6 bacterial isolates, 3 isolates showed that Maximum PSI was observed by PSB_1 (5.092) followed by PSB_3 (4.65) and PSB_4 (4.45). The bacterial isolates produced the largest halos of approximately 5.0 mm–15.1 mm within 5 days of incubation. This indicates the phosphate solubilization capacities of the isolates. This result was in agreement as reported by Anzuay et al. (2013) and Pandey et al. (2006).

3.2. Morphological and biochemical analysis of bacterial isolate

To identify the strain of the isolated PSB, morphological and biochemical tests were conducted. Morphological characterization of three PSB showing a larger clear halo zone around its colony was performed, and characteristically, all the isolates were round raised colonies and of rod-shaped, motile, and most of with shiny surface, and Isolates PSB_1 and PSB_4 were Gram-negative while PSB_3 Gram-positive (Table 4). The isolates were further characterized by a series of biochemical reactions such as Citrate utilization, Catalase Test, Indole test, Urease test, Voges-Proskauer (VP) test, and Methyl Red (MR) test to determine phenotypic properties of the isolate, and the results were summarized in Table 4.

All 3 bacteria have shown negativity for the urease and MR test. Bacteria isolate PSB_1 and PSB_3 were negative for the Citrate and indole test. However, bacteria isolate PSB_4 was positive for VP, Citrate, and indole test. The morphological and biochemical test results of PSB_1 are consistent with the many phenotypic characteristics of the genus *Pseudomonas* (Paul and Sinha, 2017), whereas PSB_3 and PSB_4 are comparable

Table 1. Independent variables and levels used in the CCD for the phosphate solubilization and IAA production of the isolate.

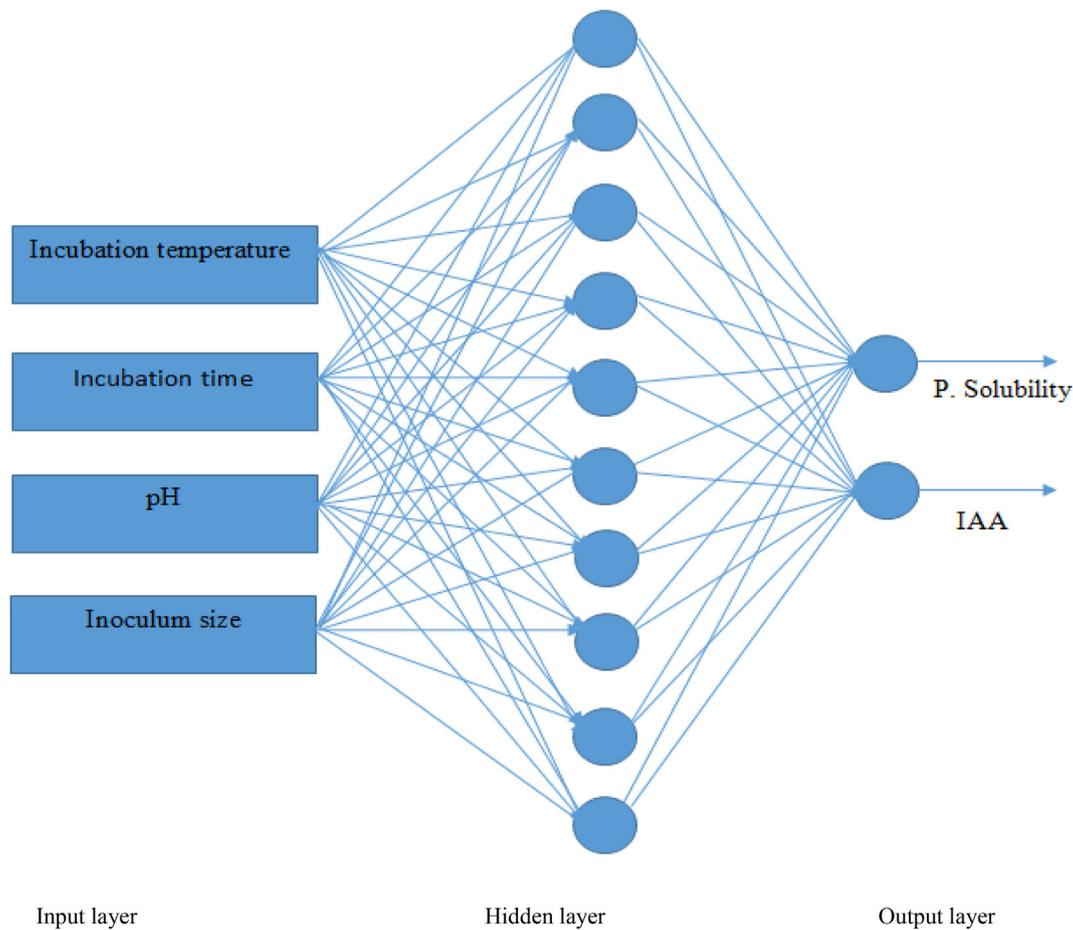| Factors	Unit	Coded symbol	Coded Levels				
			-α	-1	0	+1	+α
Incubation Temperature	°C	A	25	30	35	40	45
Incubation time	days	B	3	6	9	12	15
pH	-	C	5	6	7	8	9
Inoculum size	OD	D	1	1.5	2	2.5	3

Figure 1. Feed-forward with the backward propagation neural network used in the current study.

Table 2. Error functions and its equations with references.

Error function	Equation	Reference
Mean-squared error	$MSE = \frac{1}{n}\sum_{i=1}^{n}(Y_{i,p} - Y_{i,e})^2$ (6)	(Wu et al., 2021)
Root mean square error	$RMSE = \sqrt{\frac{\sum_{i=1}^{n}(Y_{i,e} - Y_{i,p})^2}{n}}$ (7)	(Nasrudin et al., 2020)
Standard error of prediction	$SEP = \frac{RMSE}{Y_e} \times 100$ (8)	(Gendy et al., 2020)
Coefficient of determination	$R^2 = 1 - \frac{\sum_{i=1}^{n}(Y_{i,p} - Y_{i,e})^2}{\sum_{i=1}^{n}(Y_{i,e} - Y_{i,p})^2}$ (9)	(Shukla et al., 2020)
Mean absolute error	$MAE = \frac{1}{n}\sum_{i=1}^{n}|Y_{i,e} - Y_{i,p}|$ (10)	(Awolusi et al., 2019)
Absolute average relative deviation	$AARD = \frac{1}{n}\sum_{i=1}^{n}\left(\left|\frac{Y_{i,p} - Y_{i,e}}{Y_{i,e}}\right|\right) x\, 100$ (11)	(Sodeifian et al., 2015)

where, $Y_{i,e}$ is the experimental data, $Y_{i,p}$ is the predicted data obtained from either RSM or ANN, Y_e is the mean value of experimental data and n is the number of the experimental data. The final network was selected based on the lowest training error and depending upon the test data.

with *Bacillus* sp. (Patel et al., 2016), and *Enterobacter* sp. (Abbas et al., 2014) respectively. As a result, the isolated PSB were determined to be *Pseudomonas* sp., Bacillus sp., and the genus Enterobacter. These sp. of bacteria were also discovered by a number of authors to be phosphate solubilizers (Deepa et al., 2010; Pande et al., 2017; Sadiq et al., 2013). Based on their PSI, PSB1 was selected for further analysis.

Table 3. Qualitative estimation of phosphate solubilization efficiency of isolates.

Bacterial Isolates	Colony diameter, mm	Halo zone diameter, mm	PSI
PSB$_1$	3.69	15.1	5.092
PSB$_2$	2.94	4.70	2.60
PSB$_3$	1.42	5.20	4.65
PSB$_4$	1.74	6.0	4.45
PSB$_5$	9.3	5.3	1.57
PSB$_6$	2.49	5.0	3.01

3.3. Modeling and prediction using RSM

The experimental results obtained from the solubility of phosphate and IAA production based on CCD are presented in Table 4. A total number of 30 experiments were performed with different combinations of process variables to investigate and optimize the influence of independent variables (incubation temperature, incubation time, pH, and inoculum size) on the responses (solubility of phosphate and IAA production).

3.4. Multiple linear regression results and analysis of the adequacy of the fitted model

In this study, the phosphate-dissolving capability and IAA production of phosphate solubilizing bacteria (*Pseudomonas* sp.) were determined and ANOVA was used to obtain the interaction between the process variables and the responses. The regression coefficients of the model for each response result of the ANOVA are summarized in Table 6. The ANOVA was statistically significant and suggested that at least one of the

Y.A. Waday et al.

Table 4. Morphological and biochemical characterization of PSB$_1$, PSB$_3$, and PSB$_4$ isolates.

Tests		Bacterial Isolate		
		PSB$_1$	PSB$_3$	PSB$_4$
Morphological	Color	Reddish	White	Cream
	Shape	Rod-shape	Rod-shape	Rod-shape
	Gram staining	-	+	-
	Motility	Motile	Motile	Motile
	Endospores formation	+	+	-
Biochemical	Indole test	-	-	+
	Catalase Test	+	+	-
	Urease test	-	-	-
	Voges-Proskauer (VP) test	-	-	+
	Methyl Red (MR) test	-	-	-
	Citrate utilization	-	-	+

parameters of the model can explain the experimental variation for solubility of phosphate and IAA production with the average response. The higher the value of F and the smaller p-value, the more significant is the corresponding coefficient. The variable with $P < 0.05$ is considered a significant parameter. The ANOVA results showed a perfect fit of the quadratic regression model (F-value of 32.12) ($p < 0.0001$) and F-value 35.31 ($p < 0.0001$) for soluble phosphate and IAA production, respectively. In this study, Both models do not show a Lack of Fit since the p-values for the lack of fit test are greater than 0.05 (0.3130 and 0.0599 for Soluble phosphate and IAA, respectively), indicating that lack of fit was not significant relative to the pure error. Therefore, the results obtained verified that the models generated were accurate enough to predict the soluble phosphate and IAA production within the range of the variables studied (Eqs. (12) and (13)). The analysis shows that for soluble phosphate, A, B, C, D, AC, AD, B^2, C^2, D^2 were found to have a significant effect on the soluble phosphate while AB, BC, BD, CD, and A^2 were not significant influence on the soluble phosphate. In the case of IAA, A, B, C, D, AC, AD, BC, BD, A^2, B^2, C^2, D^2 were found to have a significant effect on the IAA, while AB and CD, were not significant (Table 6).

From the results, the regression model found to be highly significant with the R^2 value of solubility of phosphate and IAA production was 0.9677, and 0.9705, respectively; indicating that the model fitted the experimental data well and the experimental error was small. Moreover, the value of the adjusted R^2 for soluble phosphate and IAA was 0.9376, and 0.9431 respectively, which confirmed that the model was highly significant, indicating good agreement between the experimental and predicted values of the dependent variables. Adjusted R^2 and predicted R^2 should be within 20% to be in good agreement as suggested by (Le Man et al., 2010). This requirement is satisfied in this study with a predicted R^2 value of soluble phosphate and IAA production was 0.8471, and 0.8436 respectively. The model, therefore, offers 84.71% and 84.36% variability in prediction solubility of phosphate and IAA production respectively beyond the experimental range of process conditions. The coefficient of variation (CV %) and standard deviation for two responses in this study were reasonably low and acceptable, showing a high degree of precision and high reliability of the conducted experiments (Table 7). Thus, the model is adequate for predictions in the range of the experimental variables.

3.5. Development of regression model equation

By applying multiple regression analysis on the experimental data, second-order polynomial equations were developed for the responses (solubility of phosphate (Y) and IAA production (X)) which can express the relationship between process variables (incubation temperature (A), incubation time (B), pH (C), and inoculum size (D)) and the responses. The final equations obtained in terms of coded factors after excluding the

insignificant terms were given in Eqs. (12) and (13), respectively. It should be noted that Eqs. (12) and (13) are only valid within the range of tested conditions: 25 °C < incubation temperature <45 °C, 3day < incubation time <15 day, 5 < pH < 9 and 1 < pH < 3.

$$\text{Phosphate solubilization (Y)} = +252.84 + 13.23A + 7.57B + 15.68C$$
$$- 9.12D - 22.96\,AC - 6.70AD - 29.04B^2$$
$$- 14.21C^2 - 24.74D^2$$

$$(12)$$

$$\text{IAA production (X)} = +79.26 + 3.30A + 1.40B + 1.31C - 1.33D$$
$$+ 2.68AC - 2.02AD + 2.31BC + 2.38BD - 6.49A^2$$
$$- 6.81B^2 - 7.02C^2 - 6.26D^2$$

$$(13)$$

The positive signs in the models signify that the concerned factor has a positive effect on the response, while the negative sign indicates that it has a negative one. According to the linear coefficients of the second-order equation, incubation temperature, incubation time, pH showed a positive effect, while, and inoculum size had a negative influence.

The Figures 2 and 3 outcomes demonstrated that the predicted values obtained from the developed model were quite close to the experimental values and lie reasonably close to the straight line and indicated the adequate agreement with the real data. The points of all predicted and experimental responses fell in 45° lines, indicating that the developed model is appropriate to predict the solubility of phosphate and IAA production. From the graph, it is clear that the values derived experimentally match closely with the developed model. Similar studies have been reported for optimization of low-cost medium for rhizobacterial strain *Pseudomonas* putida Rs-198 culture isolated from salinized soils (Peng et al., 2014) and rhizobacterial strains isolated from Acacia cyanophylla root nodules (Lebrazi et al., 2020).

3.6. Response surface analysis

To visualize and study the interactive relationship between the response and process parameters, three-dimensional (3D) surface plots were generated from the fitted polynomial equation. The 3D response
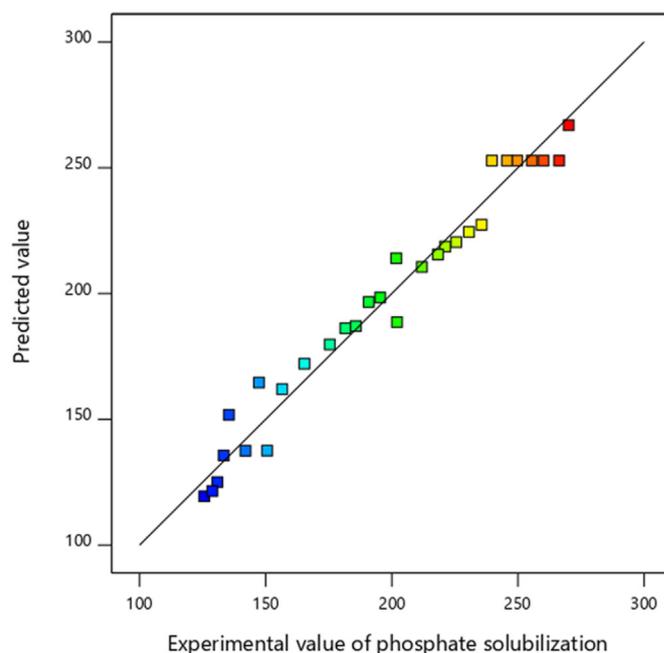
Figure 2. The curve of actual values as a function of predicted soluble phosphate.
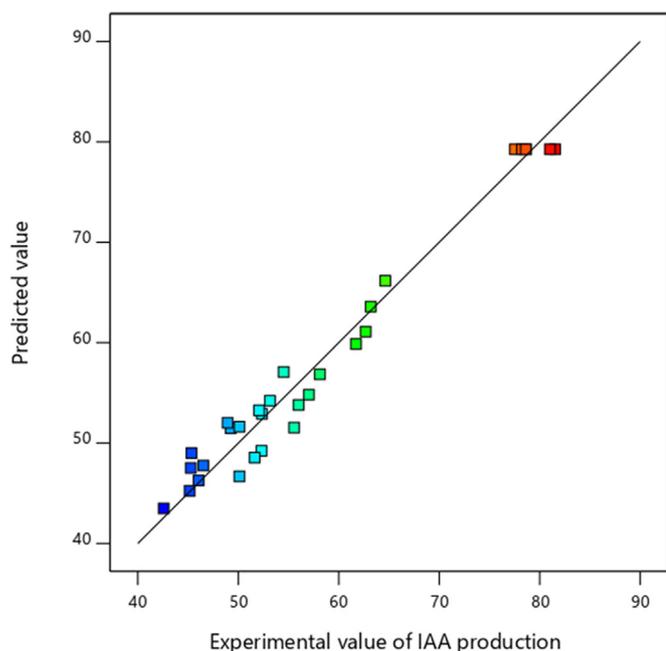
Figure 3. The curve of actual values as a function of predicted IAA production.

surfaces plots were drawn to illustrate the most significant interactive effects of the independent variables on the solubility phosphate and IAA production. The most significant parameters on each response are demonstrated in Figures 4 and 5 through 3D response surface plots. In these plots, the two factors are held constant at the optimum level, whereas the other two factors are varied within their experimental ranges.

3.7. Effect of process variables on the phosphate solubilization

Table 5 shows the phosphate solubilization values obtained from *Pseudomonas* bacteria isolated from the rhizospheric soil of coffee plants, according to the CCD matrix, with corresponding process variables. Solubility of phosphate obtained in this experiment was found to be in the range of 125.67 µg/ml - 270.12 µg/ml (Table 5), which is comparable to the phosphate solubilizing bacteria (PSB) isolated from the

rhizosphere of *Allium hookeri* Thwaites (124.8–266.4 µg/mL) (Kshetri et al., 2018) and higher than phosphate solubilizing bacteria (PSB) isolated from rhizobacterial salinized soils (44.00–63.90 mg/L) (Peng et al., 2014) (see Table 8).

Phosphate solubilization was directly proportional to incubation temperature, incubation time, and pH, and indicated that increasing any of those parameters would result increase the phosphate solubilization until the optimum value was achieved (Eq.12). The solubility of phosphate always increased if incubation temperature, incubation time, and pH increased (with constant inoculum size) (Figure 4 A), because each of these factors increases the solubility of phosphate, giving suitable conditions of medium composition required by most of the bacterial growth in bio fertilizer formulation. However, further increase in incubation temperature, incubation time, and pH resulted in a decrease of phosphate solubilization activity since too high those variables would lead to a reduction in the effectiveness of the bacterial population to affect phosphate release from the tricalcium phosphate (TCP) substrate. The pH has the most significant effect on the solubility of phosphate whose F value is 43.96, followed by incubation temperature, inoculum size, and incubation time (Table 6). The pH was directly proportional to the solubility of phosphate and indicated that increasing the value of pH would result in an increasing percentage of solubility of phosphate (Eq.12). A similar effect was noted in the phosphate solubilizing activity of bacterial sp from solid-state culture (Pande et al., 2017). The solubility of phosphate decreases with increasing inoculum size, this is might be due to the amount of phosphate was immobilized by the bacteria (Figure 4 B). The effect of inoculum size in this study is similar to previous work of (Davis et al., 2005). The result shows that the phosphate solubilizing activities increase with an increase in incubation time this suggesting that there was the microbial mobilization of phosphate during this period of incubation time.

The incubation temperature, incubation time, pH, and inoculum size show a significant ($p < 0.0001$) effect on the solubility of phosphate. The solubility of phosphate increases as the incubation time increased until optimum values are achieved. However, as the incubation time increased beyond the optimum value the solubility of phosphate decreased. This reduction is may be due to the availability of a soluble form of phosphate, which has an inhibitory effect on further phosphate solubilization and the formation of an organophosphate compound induced by organic metabolites released, which in turn, reduce the amount of available phosphate (Elhaissoufi et al., 2020).

Based on the results of the experiment conducted, it was observed that there is a negative interaction effect of incubation temperature with
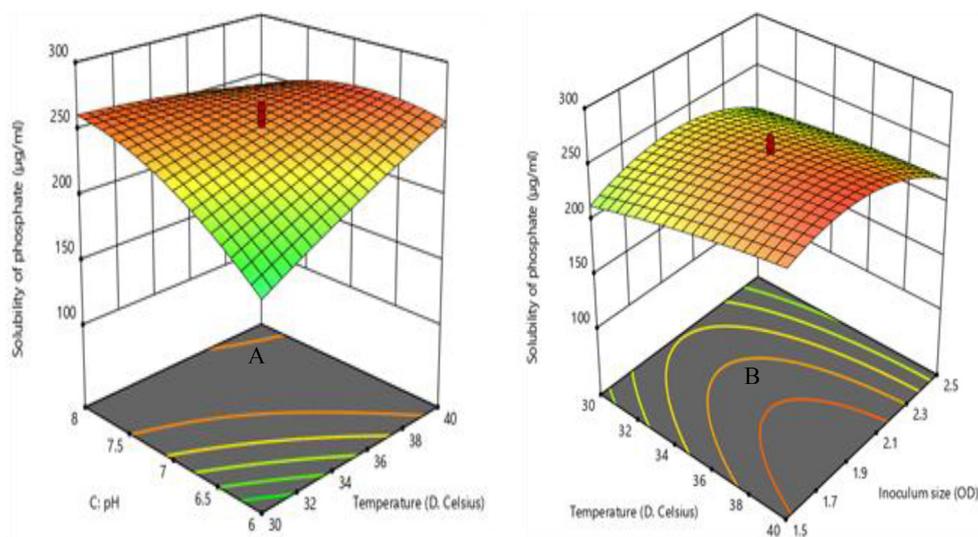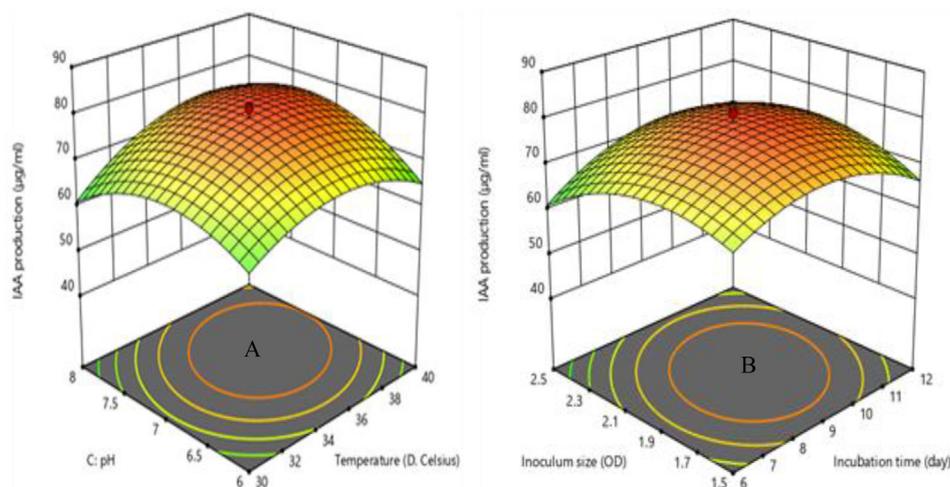

Figure 4. 3D response surface plots for solubility phosphate: (A) as the function of incubation temperature and pH at constant incubation time and (B) as the function of incubation temperature and inoculum size at constant pH and incubation time.

Figure 5. 3D response surface plot of IAA production: (A) as the function of incubation temperature and pH at constant incubation time and inoculum size and (B) as the function of incubation time and inoculum size at constant pH and incubation temperature.

pH and incubation temperature with inoculum size have a significant (p < 0.05) effect on the solubility of phosphate (Table 6). Figure 4 A shows a 3D response surface plot of the solubility of phosphate as a function of incubation temperature and pH at a fixed incubation time and inoculum size. The interaction between incubation temperature and pH has the

most significant effect on the solubility of phosphate (Table 6). The solubility of phosphate was observed to rapidly decrease with an increased pH compared to that of incubation temperature (Figure 4 A). Increasing the combined effect between incubation temperature and pH generally decreased the solubility of phosphate; the highest solubility was achieved

Table 5. Composite design matrix and experimental yields.

Run	Coded variable					Decoded Variable				Dependent Variable	
	A	B	C	D	Temp (°C)	Time (day)	pH	Inoculum Size (OD)	Soluble P (μg/ml)	IAA (μg/ml)
1	0	0	0	0	35	9	7	2	239.68	78.23
2	1	-1	-1	1	40	6	6	2.5	181.62	46.05
3	-1	-1	-1	-1	30	6	6	1.5	130.85	53.16
4	-1	1	-1	-1	30	12	6	1.5	150.58	45.16
5	1	1	1	1	40	12	8	2.5	175.44	63.18
6	-α	0	0	0	25	9	7	2	201.75	50.12
7	0	α	0	0	35	15	7	2	135.43	57.03
8	1	-1	1	-1	40	6	8	1.5	195.41	62.68
9	1	1	-1	-1	40	12	6	1.5	218.31	52.36
10	-1	1	1	1	30	12	8	2.5	225.53	52.07
11	0	0	0	0	35	9	7	2	266.34	78.62
12	0	-α	0	0	35	3	7	2	128.85	52.31
13	-1	-1	1	-1	30	6	8	1.5	190.83	45.28
14	0	0	0	α	35	9	7	3	133.38	55.56
15	0	0	0	0	35	9	7	2	260.14	81.02
16	0	0	A	0	35	9	9	2	235.59	56.01
17	1	-1	1	1	40	6	8	2.5	156.56	45.34
18	A	0	0	0	45	9	7	2	270.12	61.72
19	0	0	0	-α	35	9	7	1	165.34	58.12
20	-1	-1	-1	1	30	6	6	2.5	125.67	49.26
21	-1	1	-1	1	30	12	6	2.5	142.01	48.95
22	0	0	0	0	35	9	7	2	255.51	81.54
23	-1	1	1	-1	30	12	8	1.5	230.57	46.52
24	-1	-1	1	1	30	6	8	2.5	185.74	42.58
25	1	1	-1	1	40	12	6	2.5	202.06	50.12
26	0	0	0	0	35	9	7	2	245.65	78.62
27	1	1	1	-1	40	12	8	1.5	211.91	64.64
28	1	-1	-1	-1	40	6	6	1.5	221.16	54.52
29	0	0	0	0	35	9	7	2	249.71	77.54
30	0	0	-α	0	35	9	5	2	147.34	51.63

Table 6. Analysis of variance for response surface quadratic model of soluble phosphate and IAA.

Source	Sum of Squares	Df	Mean Square	F-value	p-value
(A) Soluble phosphate					
Model	60323.45	14	4308.82	32.12	<0.0001
A-Temperature	4198.41	1	4198.41	31.29	<0.0001
B-Inoculum time	1376.07	1	1376.07	10.26	0.0059
C-pH	5897.88	1	5897.88	43.96	<0.0001
D- Inoculum size	1996.73	1	1996.73	14.88	0.0015
AB	245.16	1	245.16	1.83	0.1965
AC	8435.96	1	8435.96	62.88	<0.0001
AD	718.64	1	718.64	5.36	0.0352
BC	234.47	1	234.47	1.75	0.2060
BD	31.16	1	31.16	0.2323	0.6368
CD	15.82	1	15.82	0.1179	0.7361
A^2	262.58	1	262.58	1.96	0.1821
B^2	23135.59	1	23135.59	172.45	<0.0001
C^2	5539.71	1	5539.71	41.29	<0.0001
D^2	16785.17	1	16785.17	125.11	<0.0001
Residual	2012.40	15	134.16		
Lack of Fit	1535.05	10	153.51	1.61	0.3130
Pure Error	477.35	5	95.47		
Cor Total	62335.85	29			
(B) IAA					
Model	4173.62	14	298.12	35.31	<0.0001
A-Temperature	260.77	1	260.77	30.88	<0.0001
B-Inoculum time	46.96	1	46.96	5.56	0.0324
C-pH	41.27	1	41.27	4.89	0.0430
D- Inoculum size	42.37	1	42.37	5.02	0.0406
AB	23.26	1	23.26	2.75	0.1177
AC	114.86	1	114.86	13.60	0.0022
AD	65.00	1	65.00	7.70	0.0142
BC	85.24	1	85.24	10.10	0.0062
BD	90.49	1	90.49	10.72	0.0051
CD	1.64	1	1.64	0.1948	0.6652
A^2	1156.37	1	1156.37	136.96	<0.0001
B^2	1270.36	1	1270.36	150.46	<0.0001
C^2	1350.93	1	1350.93	160.00	<0.0001
D^2	1075.90	1	1075.90	127.43	<0.0001
Residual	126.65	15	8.44		
Lack of Fit	113.51	10	11.35	4.32	0.0599
Pure Error	13.13	5	2.63		
Cor Total	4300.27	29			

Table 7. Regression coefficients of the predicted second-order model for the response variables.

S. No	Response parameter	Soluble phosphate	IAA production
1	Std. Dev.	11.58	2.91
2	Mean	195.97	58.00
3	C.V%	5.91	5.01
4	R^2	0.9677	0.9705
5	Adjusted R^2	0.9376	0.9431
6	Predicted R^2	0.8471	0.8436
7	Adeq Precision	18.010	17.4029
8	Model suggested	Quadratic	Quadratic

Table 8. Validation data set for experimentally determined ANN and RSM predicted values of solubility of phosphate (µg/ml) and IAA production (µg/ml).

Exp. No	Solubility of phosphate (µg/ml)			IAA production (µg/ml)		
	Experimental	Predicted value		Experimental	Predicted value	
		RSM	ANN		RSM	ANN
1	239.68	252.84	238.46	78.23	79.26	78.22
2	181.62	186.21	180.28	46.05	46.29	46.05
3	130.85	125.05	129.45	53.16	54.24	53.12
4	150.58	137.58	148.78	45.16	45.25	45.17
5	175.44	179.76	175.36	63.18	63.59	63.18
6	201.75	214.01	205.61	50.12	46.70	49.89
7	135.43	151.81	134.91	57.03	54.84	56.89
8	195.41	198.42	195.02	62.68	61.10	62.18
9	218.31	215.53	218.24	52.36	52.93	52.36
10	225.53	220.46	225.56	52.07	53.26	53.07
11	266.34	252.84	264.65	78.62	79.26	79.63
12	128.85	121.52	127.63	52.31	49.24	51.45
13	190.83	196.66	190.05	45.28	47.53	45.56
14	133.38	135.64	133.78	55.56	51.55	54.65
15	260.14	252.84	259.78	81.02	79.26	80.98
16	235.59	227.34	237.12	56.01	53.81	56.25
17	156.56	161.99	156.75	45.34	49.01	46.12
18	270.12	266.91	270.08	61.72	59.88	60.98
19	165.34	172.13	164.43	58.12	56.87	58.06
20	125.67	119.41	123.96	49.26	51.50	50.54
21	142.01	137.52	141.26	48.95	52.02	49.03
22	255.51	252.84	255.46	81.54	79.26	80.56
23	230.57	224.50	229.59	46.52	47.77	47.17
24	185.74	187.04	185.64	42.58	43.50	43.00
25	202.06	188.66	200.12	50.12	51.64	50.65
26	245.65	252.84	246.96	78.62	79.26	78.16
27	211.91	210.60	211.91	64.64	66.17	66.37
28	221.16	218.66	221.16	54.52	57.09	54.29
29	249.71	252.84	248.85	77.54	79.26	77.36
30	147.34	164.64	146.56	51.63	48.57	50.16

3.8. The effect of process variables on the indole acetic acid (IAA) production

In the present study, the produced IAA within the range of 42.58–81.54 µg/ml (Table 5), which is comparable to the phosphate solubilizing bacteria (PSB) isolated from the rhizosphere of medicinal plant *Stevia rebaudiana* (34–91.7 µg/ml) (Chandra et al., 2018) and higher than phosphate solubilizing bacteria (PSB) isolated from rhizobacterial salinized soils (44.00–63.90 mg/L) (Peng et al., 2014).

In this study, IAA is found to be significantly affected by all linear process variables (Equation 13). Based on the ANOVA, the IAA production was significantly affected by linear, interactions and quadratic between process variables. Incubation temperature, incubation time, pH, and inoculum size showed significant ($p < 0.05$) effects on the IAA production (Eq. 13). The IAA production was positively influenced by incubation temperature, incubation time, and pH. The results obtained from the ANOVA showed that incubation temperature has the most significant effect on the IAA production, followed by incubation time, inoculum size, and pH. Regarding the incubation time, linear effects were verified to be statistically significant for IAA production, as indicated by the p-value in Table 6.

The interactions among the four parameters investigated for the IAA production were examined using 3D surface plots (Figure 5 A and B). The interaction between incubation temperature and pH exhibited a strong significant ($p < 0.05$) effect on the IAA production. It can be seen from Figure 5 (A and B) that the response surface of the interaction of

when both variables were at the minimum point. This shows that the solubility of phosphate reduces with an increased interaction effect of incubation temperature with pH.

incubation temperature with pH and incubation time with inoculum size for IAA production has a steep slope, indicating significant interaction between the two factors. Significant interaction indicates that the factors work independently, whilst the presence of interaction indicates that the difference in IAA production at different levels of a factor is not the same at all levels of another factor. From F value and P-value in Table 4, it can be concluded that the order of influence of interaction term on the IAA production is: AC > BD > BC > and AD. The quadratic of incubation temperature, incubation time, pH, and inoculum size has a significant effect on the IAA production. The quadratic of pH has the most significant effect on the IAA production whose F value is 160.00 (Table 6). Similar findings were reported by another researcher (Baliyan et al., 2021).

Figure 5 (A) shows a 3D response surface plot of the IAA production as a function of incubation temperature and pH at fixed incubation time and inoculum size. RSM plot showed that IAA production increased with temperature and pH up to an optimum point where further increase in temperature or pH resulted in a decrease of IAA production activity.

3.9. Artificial neural network-based modeling

The network used in this study consists of four input neurons (incubation temperature, pH, incubation time, and inoculum size) in the first layer, two output neurons (solubility of phosphate and IAA production) in the third layer, and 10 hidden neurons are shown in Figure 6a. Figure 6b shows the scatter diagrams that compared the actual versus the computed neural network data for training, testing and validation networks. The correlation coefficients (R) values for training (0.99913), test (0.9802), validation (0.98834), and whole data sets (0.99268) indicating that the ANN model shows better regression and fitting compared to the RSM model. Nearly the whole point has been scattered around the 45° line an indication of excellent compatibility between the experimental results and ANN predicted output data values. As can be seen from Figure 6b the ANN model indicating that prediction for training, validation, and testing has sufficient reliability and can be used for predicting the solubility of phosphate (µg/ml) and IAA production (µg/ml).
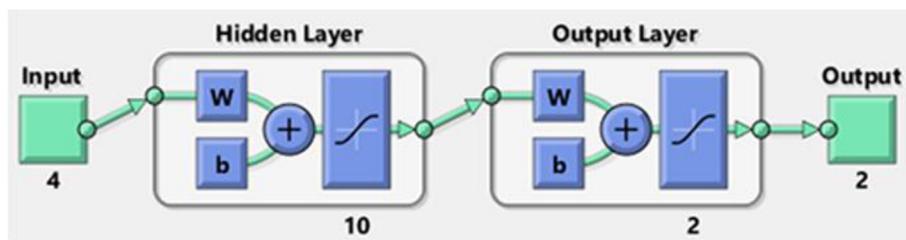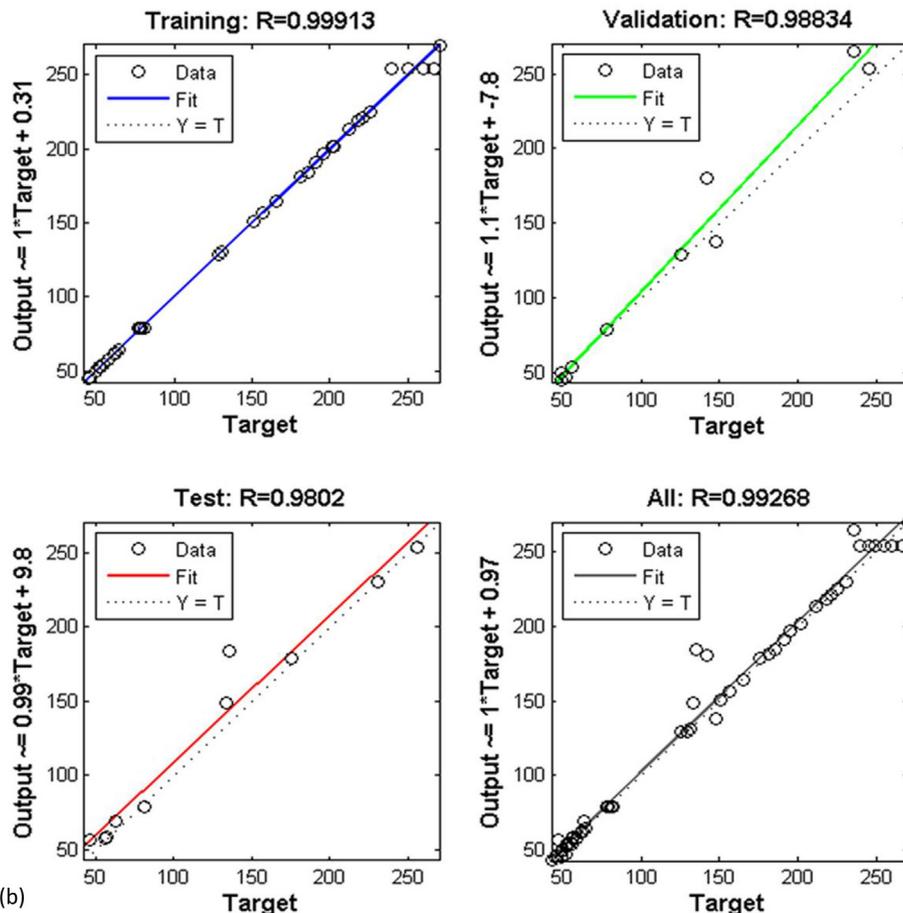
Figure 6. Network architecture (a), correlation plots of predicted versus experimental values for the developed ANN model with training, validation, test and all prediction set (b).

Table 9. Comparison of predictive abilities of RSM and ANN models.

	Solubility of phosphate (µg/ml)		IAA production (µg/ml)	
Parameters	RSM	ANN	RSM	ANN
RMSE	8.190	1.205	2.054	1.686
R^2	0.968	0.999	0.971	0.979
AARD (%)	0.961	0.487	3.234	2.532
MAE	6.863	0.877	1.776	1.396
SEP	4.179	0.615	3.541	2.907
MSE	67.077	1.452	4.219	2.842

3.10. Performance assessment of the predictive capability of the developed models

The effectiveness of the developed RSM and ANN models to predict the solubility of phosphate and IAA production were statistically measured, in terms of the RMSE, R^2, MSE, SEP, MAE, and AARD. The value of R^2 should be close to 1 for a good correlation between experimental and predicted values and also indicating a good fit of the model. The values obtained RMSE for both were all low (Table 9), supporting a good fit of the models. The high values of R^2 as well as the lower the values of these statistical indicators, obtained for the responses signify good fitting between the experimental and predicted values. The results showed that both models performed reasonably well, but ANN models have the more powerful modeling capability compared to the RSM model for both solubility of phosphate and IAA production. As can be observed, the ANN predicted value is much closer to that of the experimentally measured data, suggesting that the ANN model has superior prediction ability than the RSM model (Table 9).

3.11. Optimization and Validation of the model by using response surface modeling

The main objectives of this study were to determine the optimal operating parameters for the maximum phosphate solubilization and production of IAA by phosphate solubilizing bacteria isolated from rhizospheric soils of the coffee plant. The numerical optimization of phosphate solubilization and production of IAA were performed by using statistical experimental design techniques. Solubility of phosphate and production of IAA was set at maximum values while the value of process variables was set in the range under study. To obtain the maximum phosphate solubilization and production of IAA, the predicted combination of process variables were as follows: incubation temperature of 37.5 °C, incubation time of 9 days, pH of 7.2, and inoculum size of 1.89 OD. Under these conditions, the model predicted solubility of phosphate of 260.69 µg/ml and production of IAA of 80.00 µg/ml with a desirability value of 0.947. To validate the optimum conditions predicted by the model using desirability ramp, triplicate experiments were performed under the predicted process conditions, and phosphate solubilization of 260.45 ± 0.31 µg/ml and production of IAA of 79.65 ± 0.87 µg/ml were obtained. The results are closely related to the data obtained from optimization analysis using desirability functions, indicating CCD incorporates with desirability function could be effectively used to optimize the parameters that affect the solubility of phosphate and production of IAA.

4. Conclusions

The results of the present study provide substantial evidence that phosphate solubilizing rhizobacteria isolated from rhizospheric soil of coffee plants facilitate solubilization of free phosphate in soil, and also enhance the growth of the plant. Six phosphate solubilizing bacteria were isolated on PVK agar media and their P dissolution efficiencies were quantified on insoluble Phosphate. Three of the best P dissolving strains were characterized using different morphological and biochemical tests and the isolate strains were identified as *Pseudomonas*, *Bacillus*, and *Enterobacter* species. *Pseudomonas* species demonstrated high P dissolving capacities (PSI = 5.092) followed by Bacillus (PSI = 4.65) and Enterobacter (PSI = 4.45). The effects of process variables (incubation temperature, incubation time, pH, and inoculum size) on Phosphate solubilization and IAA production by *Pseudomonas* species is further studied to obtain the optimum operating conditions. The performance of both the models was compared based on prediction accuracy of the solubility of phosphate and production of IAA. The study revealed that all four variables linearly affect the solubility of phosphate and the production of IAA. Based on the values of R^2, RMSE, SEP, MSE, MAE, and AARD for validation data sets, the ANN model was demonstrated to be more efficient than the RSM model both in data fitting and prediction capabilities. The finding of the study indicated that incubation temperature of 37.5 °C, incubation time of 9 days, pH of 7.2, and inoculum size of 1.89 OD is the best combination of process parameters that result the highest phosphate solubilization of 260.45 µmg/ml and production of IAA of 79.65 µg/ml. The effect of inoculation of PSB with TCP was more pronounced to enhance the growth of the plant. The significant increase in the P content of PSB-treated plants emphasizes the potential of an economically and eco-friendly means of achieving higher levels of phosphorus. This result will help facilitate further research on the ability of this bacterium to solubilize other phosphate sources and also help highlight the need for molecular identification of the isolate and its use as a plant bio fertilizer.

References

Abbas, S.Z., Rafatullah, M., Ismail, N., Lalung, J., 2014. Isolation, identification, characterization, and evaluation of cadmium removal capacity of Enterobacter species. J. Basic Microbiol. 54, 1279–1287.

Aklilu, E.G., 2021. Modeling and optimization of pectin extraction from banana peel using artificial neural networks (ANNs) and response surface methodology (RSM). J. Food Meas. Char. 15, 2759–2773.

Alemu, A., Abebe, G., Tsegaye, W., Golassa, L., 2011. Climatic variables and malaria transmission dynamics in Jimma town, South West Ethiopia. Parasites Vectors 4, 1–11.

Anbalagan, P., Krishnaswamy, V.G., 2017. Optimisation of growth factors for effective use of phosphate solubilizing bacterial strains and its use as bioinoculants for the growth of groundnut (Arachis hypogaea) plant. Biotechnol. J. Int. 19, 1–16.

Anzuay, M.S., Ciancio, M.G.R., Ludueña, L.M., Angelini, J.G., Barros, G., Pastor, N., Taurian, T., 2017. Growth promotion of peanut (Arachis hypogaea L.) and maize (Zea mays L.) plants by single and mixed cultures of efficient phosphate solubilizing bacteria that are tolerant to abiotic stress and pesticides. Microbiol. Res. 199, 98–109.

Anzuay, M.S., Frola, O., Angelini, J.G., Ludueña, L.M., Fabra, A., Taurian, T., 2013. Genetic diversity of phosphate-solubilizing peanut (Arachis hypogaea L.) associated bacteria and mechanisms involved in this ability. Symbiosis 60, 143–154.

Awolusi, T.F., Oke, O.L., Akinkurolere, O.O., Atoyebi, O.D., Awolusi, T.F., Oke, O.L., Akinkurolere, O.O., 2019. Comparison of response surface methodology and hybrid-training approach of artificial neural network in modelling the properties of concrete containing steel fibre extracted from waste tyres. Cogent Eng. 6, 1–18.

Baliyan, N., Dhiman, S., Dheeman, S., Kumar, S., 2021. Optimization of Indole-3-acetic acid using response surface methodology and its effect on vegetative growth of chickpea Rhizosphere Optimization of indole-3-acetic acid using response surface methodology and its effect on vegetative growth of chickpea. Rhizosphere 17, 100321.

Banerjee, A., Varshney, D., Kumar, S., Chaudhary, P., Gupta, V.K., 2017. Biodiesel production from castor oil : ANN modeling and kinetic parameter estimation. Int. J. Integrated Care 8, 253–262.

Chandra, S., Askari, K., Kumari, M., 2018. Optimization of indole acetic acid production by isolated bacteria from Stevia rebaudiana rhizosphere and its effects on plant growth. J. Genet. Eng. Biotechnol. 16, 581–586.

Davis, K.E.R., Joseph, S.J., Janssen, P.H., 2005. Effects of growth medium, inoculum size, and incubation time on culturability and isolation of soil bacteria. Appl. Environ. Microbiol. 71, 826–834.

Deepa, C.K., Dastager, S.G., Pandey, A., 2010. Isolation and characterization of plant growth promoting bacteria from non-rhizospheric soil and their effect on cowpea (Vigna unguiculata (L.) Walp.) seedling growth. World J. Microbiol. Biotechnol. 26, 1233–1240.

Elhaissoufi, W., Khourchi, S., Ibnyasser, A., Ghoulam, C., Rchiad, Z., Zeroual, Y., Lyamlouli, K., Bargaz, A., 2020. Phosphate solubilizing rhizobacteria could have a stronger influence on wheat root traits and aboveground physiology than rhizosphere P solubilization. Front. Plant Sci. 11, 1–15.

Gendy, T.S., Ghoneim, S.A., Zakhary, A.S., 2020. Comparative appraisal of response surface methodology and artificial neural network method for stabilized turbulent confined jet diffusion flames using bluff-body burners. World J. Eng. Technol. 8, 121–143.

Gordon, S.A., Weber, R.P., 1951. Colorimetric estimation of indole acetic acid. Plant Physiol. 26, 192–195.

Holt, D.H.B.J.G., 1994. Bergey's Manual of Determinative Bacteriology, 9th. Williams & Wilkins, Baltimore.

Isenberg, H.D., 1998. Essential Procedures for Clinical Microbiology. American Society for Microbiology (ASM).

Kalayu, G., 2019. Phosphate solubilizing microorganisms: promising approach as biofertilizers. Int. J. Agron. 1–7.

Kshetri, L., Pandey, P., Sharma, G.D., 2018. Rhizosphere mediated nutrient management in Allium hookeri Thwaites by using phosphate solubilizing rhizobacteria and tricalcium phosphate amended soil Rhizosphere mediated nutrient management in Allium hookeri Thwaites by using phosphate solubilizing rhi. J. Plant Interact. 9145, 256–269.

Le Man, H., Behera, S.K., Park, H.S., 2010. Optimization of operational parameters for ethanol production from Korean food waste leachate. Int. J. Environ. Sci. Technol. 7, 157–164.

Lebrazi, S., Niehaus, K., Bednarz, H., Fadil, M., Chraibi, M., Fikri-Benbrahim, K., 2020. Screening and optimization of indole-3-acetic acid production and phosphate solubilization by rhizobacterial strains isolated from Acacia cyanophylla root nodules and their effects on its plant growth. J. Genet. Eng. Biotechnol. 18, 1–12.

Midekssa, M.J., Löscher, C.R., Schmitz, R.A., Assefa, F., 2015. Characterization of phosphate solubilizing rhizobacteria isolated from lentil growing areas of Ethiopia. Afr. J. Microbiol. Res. 9, 1637–1648.

Mohd Yusoff, A.S., Zulkefly, S., Adekunle Salisu, M., Ahmad Kamil, M.J., 2017. Optimization of liquid medium for high phosphate solubilization by Serratia marcescens strain AGKT4. Turk. J. Agric. Food Sci. Technol. 5, 1626.

Monzón, L., Villanueva, E., 2021. Ultrasound-assisted extraction of polyphenols from avocado residues : modeling and optimization using response surface methodology and artificial neural networks. Scientia Agropecuaria Web 12, 33–40.

Muleta, D., Assefa, F., Börjesson, E., Granhall, U., 2013. Phosphate-solubilising rhizobacteria associated with Coffea arabica L. in natural coffee forests of southwestern Ethiopia. J. Saudi Soc. Agric. Sci. 12, 73–84.

Nasrudin, N.A., Jewaratnam, J., Hossain, M.A., Ganeson, P.B., 2020. Performance comparison of feedforward neural network training algorithms in modelling microwave pyrolysis of oil palm fibre for hydrogen and biochar production. Asia Pac. J. Chem. Eng. 15, 1–16.

Pande, A., Pandey, P., Mehra, S., Singh, M., Kaushik, S., 2017. Phenotypic and genotypic characterization of phosphate solubilizing bacteria and their efficiency on the growth of maize. J. Genet. Eng. Biotechnol. 15, 379–391.

Pandey, A., Trivedi, P., Kumar, B., Palni, L.M.S., 2006. Characterization of a Phosphate Solubilizing and Antagonistic Strain of Pseudomonas putida (B0) Isolated from a Sub-Alpine Location in the Indian Central Himalaya, 53, pp. 102–107.

Patel, G., Singh, S., Saxena, D.S.K., Kaur, D.K.J., 2016. Isolation, biochemical characterization and production of biofertilizer from Bacillus megaterium. Int. J. Life Sci. Sci. Res. 2.

Paul, D., Sinha, S.N., 2017. Isolation and characterization of phosphate solubilizing bacterium Pseudomonas aeruginosa KUPSB12 with antibacterial potential from river Ganga, India. Ann. Agrarian Sci. 15, 130–136.

Peng, Y., He, Y., Wu, Z., Lu, JLiC., 2014. Screening and optimization of low-cost medium for Pseudomonas putida Rs-198 culture using RSM. Braz. J. Microbiol. 45, 1229–1237.

Sadiq, H.M., Jahangir, G.Z., Nasir, I.A., Iqtidar, M., Iqbal, M., 2013. Isolation and characterization of phosphate-solubilizing bacteria from rhizosphere soil. Biotechnol. Biotechnol. Equip. 27, 4248–4255.

Sharon, J.A., Hathwaik, L.T., Glenn, G.M., Imam, S.H., Lee, C.C., 2016. Isolation of efficient phosphate solubilizing bacteria capable of enhancing tomato plant growth. J. Soil Sci. Plant Nutr. 16, 525–536.

Shukla, V., Bandyopadhyay, M., Pandya, V., Maulik, A.P.A., 2020. Artificial neural network based predictive negative hydrogen ion helicon plasma source for fusion grade large sized ion source. Eng. Comput.

Sodeifian, G., Sajadian, S.A., Ardestani, N.S., 2015. Evaluation of the response surface and hybrid artificial neural network-genetic algorithm methodologies to determine extraction yield of Ferulago angulata through supercritical fluid. J. Taiwan Inst. Chem. Eng. 1–9.

Somasegaren, P., Hoben, H.J., 1994. Quantifying the growth of rhizobia. In: Garber, R. (Ed.), Handbook for Rhizobia: Methods in LegumeRhizobia Technology. Springer, New York.

Watanabe, F.S., Olsen, S.R., 1965. Test of an ascorbic acid method for determining phosphorus in water and NaHCO extracts from soil. Soil Sci. Soc. Am. J. 29, 677–678.

Wu, S., Yang, J., Cao, G., 2021. Prediction of the Charpy V-notch impact energy of low carbon steel using a shallow neural network and deep learning. Int. J. Miner. Metall. Mater.

Yu, A., Liu, Y., Li, X., Yang, Y., Zhou, Z., Liu, H., 2021. Modeling and optimizing of NH4+ removal from stormwater by coal-based granular activated carbon using RSM and ANN coupled with GA. Water 13, 608.